Journal of Molecular Structure 1118 (2016) 288–292

Contents lists available at ScienceDirect

Journal of Molecular Structure

journal homepage: http://www.elsevier.com/locate/molstruc

X-Ray diffraction, spectroscopy and thermochemical characterization of the pharmaceutical paroxetine nitrate salt

Paulo S. Carvalho Jr. [a], Cristiane C. de Melo [a, b], Alejandro P. Ayala [b], Javier Ellena [a, *]

[a] Instituto de Física de São Carlos, Universidade de São Paulo, CP 369, 13560-970, São Carlos, SP, Brazil
[b] Departamento de Física, Universidade Federal do Ceará, CP 6030, Fortaleza, Ceará 60455–970, Brazil

ARTICLE INFO

Article history:
Received 4 March 2016
Received in revised form
5 April 2016
Accepted 6 April 2016
Available online 14 April 2016

Keywords:
Antidepressant
Paroxetine nitrate
Solid state
DSC/TGA
Infrared spectra

ABSTRACT

A comprehensive solid state study of Paroxetine nitrate hydrate, $(PRX^{+}\cdot NO_3^{-})H_2O$, is reported. This salt was characterized by a combination of methods, including Single crystal X-ray diffraction, Thermal analysis, Fourier transform infrared spectroscopy (FTIR) and Solubility measurements. $(PRX^{+}\cdot NO_3^{-})H_2O$ crystallizes in the monoclinic C2 space group ($Z' = 1$) and its packing was analyzed in details, showing that the main supramolecular motif consists in a $C_2^2(4)$ chain formed by charge-assisted N^{+}-H···O^{-} hydrogen bonds. The salt formation and conformation features were also accuracy established *via* FTIR spectra. In comparison with the pharmaceutical approved $(PRX^{+}\cdot Cl^{-})\cdot 0.5H_2O$, $(PRX^{+}\cdot NO_3^{-})\cdot H_2O$ showed a decrease of 24 °C in the drug melting peak and a slight reduction in its water solubility value.

1. Introduction

Paroxetine (PRX), [(3S-trans)-3-[(1,3-benzodioxol-5-yloxy) methyl]-4-(4-fluorophenyl)-piperidine (Scheme 1), is the most potent inhibitor of the neuronal reuptake of serotonin (5-hydroxytryptamine, 5-HT) [1] and is clinically approved for the treatment of major depression, obsessive compulsive disorder, generalized anxiety and social phobia [1–7]. Furthermore, PRX is well tolerated and effective in the depression/anxiety treatment of young and elders [2], being one of the most widely prescription drugs in the world [8]. PRX has been pharmaceutically administered as a hydrochloride salt. Two polymorphic forms are recognized for this salt: a stoichiometric hydrate, $(PRX^{+}Cl^{-})H_2O$, and a hemihydrate form, $(PRX^{+}Cl^{-})0.5H_2O$; in which the latter is the thermodynamically most stable. Additionally, anhydrate [9] and solvate salts containing propan-2-ol (isopropyl alcohol) [10] has been reported. Recently, Paroxetine bromide hemihydrate, $(PRX^{+}Br^{-})0.5H_2O$ and its corresponding dehydrate phase have been reported for us, as a part of our studies on designing of better antidepressant solid forms [11]. Beyond these structures, novel PRX salts with improved solubility and stability are still requested to provide a better manufacturing and pharmaceutical performance of this drug.

Salt selection is a common strategy applied to improve pharmaceutical properties of ionic APIs. In general, the salt confers valuable attributes such as the increasing of chemical stability, aqueous solubility and bioavailability [12–15]. For this purpose, there are a wide variety of salt formers included into the GRAS list with different chemical properties (pK_a, molecular weight, solubility) that can be combined with PRX to achieve a salt. Within this context, we have been rationally prepared the paroxetine nitrate hydrate salt, $(PRX^{+}\cdot NO_3^{-})H_2O$, following a supramolecular approach based on the establishment of charge-assisted hydrogen bonds (CAHBs). Structural correlations between $(PRX^{+}\cdot NO_3^{-})H_2O$, $(PRX^{+}Cl^{-})H_2O$ and $(PRX^{+}Cl^{-})0.5H_2O$ salts were also accuracy established. Furthermore, thermal behavior, spectroscopy properties and solubility measurements were performed for supporting the crystallographic results.

2. Experimental details

2.1. Preparation of paroxetine nitrate salt

Paroxetine chloride hemihydrate, $(PRX^{+}Cl^{-})0.5H_2O$, was used as a precursor for the synthesis of the nitrate salt. Chemicals and solvents, such as sodium hydroxide, sodium sulfate anhydrous,

* Corresponding author.
E-mail address: javiere@ifsc.usp.br (J. Ellena).

http://dx.doi.org/10.1016/j.molstruc.2016.04.014
0022-2860/

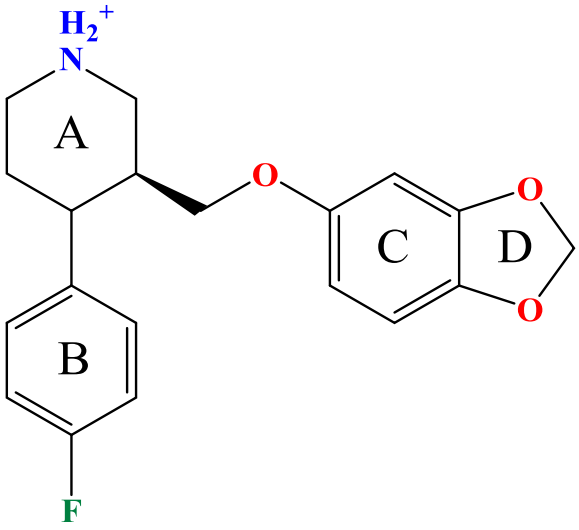

Scheme 1. Structure of Paroxetine cation (PRX^+). The N1–C1→C5, C7→C12, C14→C19 and C10–C11–O5–C13–O6 are designed A, B, C and D rings, respectively.

nitric acid, ethanol 95%, ethyl ether were of reagent grade quality and used without further purification. Paroxetine free base was obtained after deprotonation of $(PRX^+Cl^-)0.5H_2O$, following a protocol previously reported for us [11]. $(PRX^+NO_3^-)H_2O$ was prepared though the reaction of PRX free base and HNO_3 acid. Single crystals were growth from an ethanol solution 95%(v/v).

2.2. Single-crystal X-ray diffraction (SCXRD)

X-ray data of $(PRX^+NO_3^-)H_2O$ were acquired at 120 K (Cryostream, Oxford Cryosystems) on a Bruker D8 VENTURE diffractometer with PHOTON 100 CMOS detector system, using Cu Kα radiation. The data were integrated and processed *via* SAINT [16] and SADABS [17] softwares. The structure was determined using the Olex2 [18] program as a graphical interface together with the SHELXS and SHELXL programs [19], in order to solve and refine the structure, respectively. Hydrogen atoms were placed in geometric positions and refined with fixed individual displacement parameters [$U_{iso}(H) = 1.2U_{eq}$ or $1.5U_{eq}$] according to the riding model (C-H bond lengths of 0.97 Å and 0.96 Å, for methylene and methyl groups, respectively). Molecular representations, tables and pictures were generated by Olex2 [18] and MERCURY 3.2 [20] programs. The crystallographic data were deposited at the Cambridge Crystallographic Data Center under the numbers CCDC 1456602. Copies of the data can be obtained, free of charge, *via* www.ccdc.cam.ac.uk.

2.3. Vibrational spectroscopies

Middle infrared spectrum (4000-400 cm^{-1}) was recorded for $(PRX^+NO_3^-)H_2O$ and $(PRX^+Cl^-)H_2O$ salts as KBr pellets on a Shimadzu IR Prestige FTIR Spectrometer. The spectra were acquired under 64 scans of accumulation and at 4 cm^{-1} of resolution.

2.4. Thermal analysis

Differential Scanning Calorimetric measurements (DSC) were carried out on a Shimadzu DSC-60 instrument. Samples (2.5 ± 0.5 mg) were sealed in a crimped aluminum pan and heated under a flow of 5% O_2-N_2 from 25 to 300 °C at a heating rate of 10 °C/min. Thermogravimetric analyses (TGA) were performed on a Shimadzu TGA-60 thermobalance. Approximately 2.5 mg of sample were placed on an alumina pan and heated under a flow of 5% O_2-N_2 from 25 to 300 °C at a heating rate of 10 °C/min. All data were processed using the Shimadzu TA-60 thermal data analysis software.

2.5. Hot-stage microscopy (HSM)

Hot-stage (HS) microscopy was performed using a Linkam T95-PE device coupled to an optical microscope Leica DM2500 P. The $(PRX^+NO_3^-)H_2O$ crystal was heated at a constant rate of 10 °C/min from 25 °C to 150 °C, with this process being stopped after the melting of the compound. Images were recorded by a CCD camera attached to the microscope in time intervals of 10 s *via* the software Linksys 32.

2.6. Solubility

Aqueous solubility of $(PRX^+NO_3^-)H_2O$ was determined by the classical saturation shake-flask method at 20 °C in deionized water [21]. A saturated solution of $(PRX^+NO_3^-)H_2O$ was obtained stirring an excess amount of $(PRX^+NO_3^-)H_2O$ salt (30 mg) in 600 μL of water for 48 h. After this time, an aliquot of the saturated solution was removed, filtered through a 0.45 mm filter (Millipore), diluted 100-fold in water and its concentration measured by UV spectroscopy at $\lambda_{max} = 293$ nm. The standard solutions used to generate the calibration curve were prepared using $(PRX^+Cl^-)0.5H_2O$ salt. The concentration of PRX^+ in the saturated aliquots was quantified by interpolating of spectroscopic measurements in a calibration curve whose concentrations ranged from 0.005 to 0.2 mg mL^{-1}. This experiment was run in triplicate.

3. Results and discussion

3.1. Crystal structure of paroxetine nitrate hydrate

Considering the strong tendency of PRX to form salts ($pK_a = 9.9$ of piperidine N), and the dominance of CAHBs in the crystal packing of chloride and bromide PRX forms [10,11,22], a stoichiometric paroxetine nitrate hydrate salt was prepared, $(PRX^+ NO_3^-)H_2O$. This salt crystallizes in the monoclinic Sohncke space group C2 in a needle-shaped morphology. The C-centered unit cell shows a very long *a* axis compared to *b* and *c*-axis. Details of the structure determination and the refinement parameters are presented in Table 1. The asymmetric unit encloses a protonated PRX^+ molecule, a NO_3^- anion and a H_2O molecule. The water molecule lies on the crystallographic 2-fold axis and had its H atoms refined with 0.5 of occupancy. A view of crystallographic asymmetric unit is shown in Fig. 1.

PRX^+ is a six-membered piperidinium ring in the usual chair conformation (puckering parameters [23]: $q_2 = 0.0284(3)$, $q_3 = -0.5705(3)$, $Q_T = 0.5713(3)$, $\varphi_2 = -52.69(5.10)$ and $\theta_2 = 177.15(3)^o$) with the ethoxyl-benzodioxole and fluorophenyl substituents in the equatorial position. The geometric parameters of PRX^+ are listed in Table S1. Due to protonation, the sp^3 hybridized N1 atom bears a positive charge and assumes a tetrahedral configuration. In the present structure, the ethoxyl bridge between the piperidine ring and benzodioxolo group (C + D ring) has an antiperiplanar conformation with C5-C6-O4-C7 of 172.2(3)° (Table S1, support information). As reported previously, the conformational flexibility of PRX^+ is related to the rotation freedom about C6-O4 bond. Additionally, the C6-O4-C7-C12 torsion angle that defines the orientation of benzodioxole groups with respect to C5-C6-O4 mean plane assumes the value of −169.2(3)°. Although the conformation of PRX^+ in $(PRX^+ NO_3^-)H_2O$ salt differs from those reported in $(PRX^+ Cl^-)0.5H_2O$ [10,22] and $(PRX^+ Br-)0.5H_2O$

Table 1
Crystal data and structure refinement of $(PRX^{+}NO_3^{-})H_2O$.

Structure	$(PRX^{+}NO_3^{-})H_2O$
Empirical formula	$C_{19}H_{21.5}FN_2O_{6.5}$
Formula weight	400.88
Temperature/K	150.0(2)
Crystal system	Monoclinic
Space group	C2
a/Å	39.7779(13)
b/Å	5.8787(2)
c/Å	7.9925(3)
β/°	97.022(2)
Volume/Å^3	1854.97(11)
Z, Z′	4, 1
ρ_{calc} g/cm^3	1.435
μ/mm^{-1}	0.979
F(000)	842.0
Crystal size/mm^3	0.562 × 0.122 × 0.06
Radiation	CuKα (λ = 1.54178)
2Θ range for data collection/°	4.476 to 140.402
Index ranges	−48 ≤ h ≤ 47 −7 ≤ k ≤ 7 −9 ≤ l ≤ 9
Reflections collected	7890
Independent reflections	3312 [R_{int} = 0.0624, R_{sigma} = 0.0670]
Data/restraints/parameters	3312/1/259
Goodness-of-fit on F^2	1.049
Final R indexes [I ≥ 2σ (I)]	R_1 = 0.0413, wR_2 = 0.0830
Final R indexes [all data]	R_1 = 0.0567, wR_2 = 0.0892
Largest diff. peak/hole/e Å^{-3}	0.17/−0.26
Flack parameter	−0.16(17)

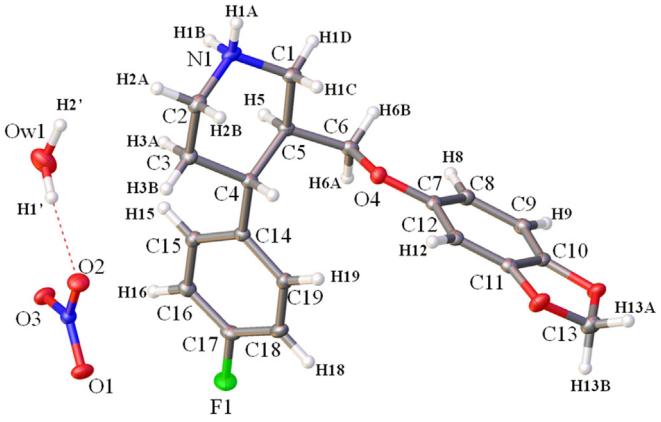

Fig. 1. Crystallographic asymmetric unit view of $(PRX^{+}NO_3^{-})H_2O$. The hydrogen atoms are label following the nomenclature of heavy atoms to which they are bonded.

hemihydrates [11], it is similar to the one found in $(PRX^{+}\ Cl^{-})H_2O$ (Fig. 2). Interestingly, only in the nitrate salt, the C13 atom is co-planar with the 1,3-dioxolane ring (D ring).

PRX nitrate is formed *via* the N1^{+}-H1A···O1^{-} CAHB (see Table S2 for H-bond geometry, Supporting Information). The PRX^{+} NO_3^{-} ionic pairs are connect to each other by N1^{+}-H1B···O3^{-} CAHB into an one-dimensional supramolecular $C_2^2(4)$ chain along the [010] direction. The ionic pairs are also stabilized by C18-H18···O5 interactions. Parallel layers of $PRX^{+}NO_3^{-}$ intercalated by H_2O channels (Fig. 3) characterize the 2-D assembly. The water molecules, in turn, stabilize the NO_3^{-} anions *via* the O1w-H1'···O2 hydrogen bonds, by reducing the electronic repulsion between the anions. Furthermore, two C-H···π interactions contribute to the overall supramolecular arrangement: C12-H12···C-ring and C13-H13B···B-ring. The directionality of C13-H13B···π is the feature that seems to corroborate with the planarity of the D ring. Also, the PRX^{+} molecule exhibits an intramolecular C19-H19···O4 interaction

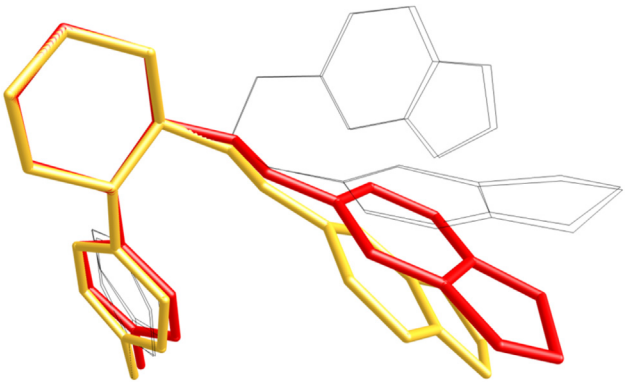

Fig. 2. The superposed of PRX^{+} molecule from different solid forms. The red molecule is from $(PRX^{+}NO_3^{-})H_2O$, the yellow one from $(PRX^{+}Cl^{-})H_2O$ [24] and black ones are from the isostructural $(PRX^{+}Cl^{-})0.5H_2O$ [10] and $(PRX^{+}Br^{-})0.5H_2O$ [11] hemihydrates.

($d_{C\ldots O}$ = 3.285(4) Å), which can explain the slight conformational differences between $(PRX^{+}NO_3^{-})H_2O$ and $(PRX^{+}Cl^{-})H_2O$ [24].

3.2. Vibrational spectra and assignments.

The analysis of the vibrational modes confirmed the conformational and supramolecular features observed in the crystallographic study. For a better understanding of the FTIR spectrum of $(PRX^{+}NO_3^{-})H_2O$, the FTIR spectrum of $(PRX^{+}Cl^{-})0.5H_2O$ is also included in Fig. 4. Analysis and band assignments were made as previously described [11,25,26].

As expected, both spectra are affected by the protonation of the secondary amine. For the nitrate salt, the band at 1345 cm^{-1}, associated to the piperidine C-N stretching mode, appears red-shifted to 1324 cm^{-1}. Another significant shift observed in the spectra of this salt, refers to the band at 803 cm^{-1}. This band arises from the coupling of phenyl-ring breathing and N-H bendings and undergoes a blue-shifted of 13 cm^{-1} (816 cm^{-1}).

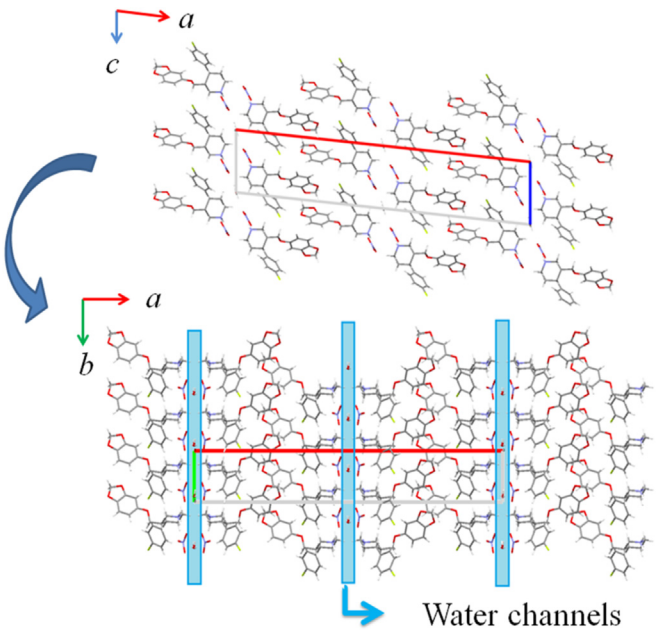

Fig. 3. Crystal packing view along the *b* and *c* axis. The blue selection indicate the water channels which the H_2O molecules are link two adjacent nitrate ions by O-H···O hydrogen bond.

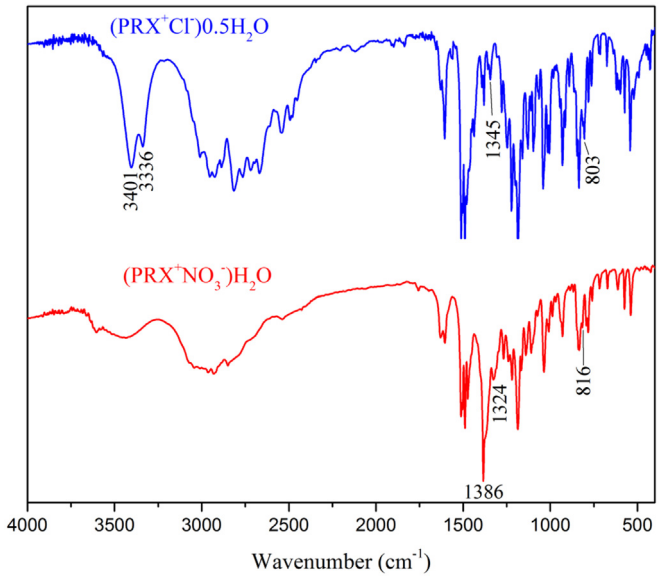

Fig. 4. FTIR spectrum of $(PRX^{+}NO_3^{-})H_2O$ and $(PRX^{+}Cl^{-})0.5H_2O$.

Unfortunately, the N-H stretching vibrations, arising from protonation of the secondary amine, only can be seen in the PRX chloride spectrum (3401 and 3336 cm^{-1}). A broad band corresponding to the water O-H stretching overlaps these two bands in PRX nitrate. Additionally, the nitrate salt also shows the presence of new bands associated to the vibrational modes of the nitrate anion. The bands at 1324 and 1386 cm^{-1}, only presented in PRX nitrate, has been assigned to the stretching mode of the N═O bonds, once PRX chloride has no absorption bands in this region.

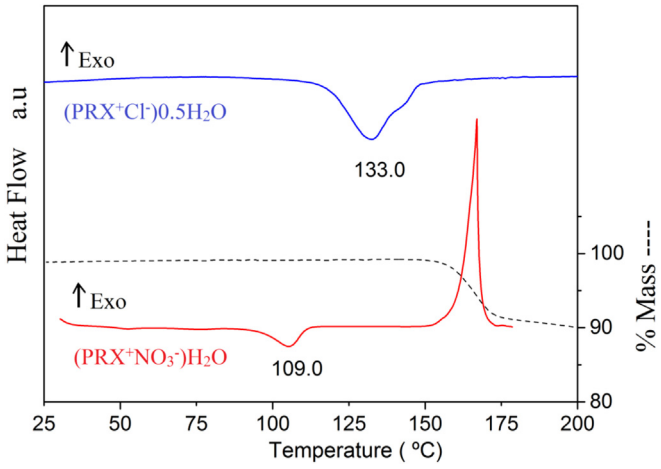

Fig. 5. DSC (line filled) and TGA (dash line) thermograms of $(PRX^{+}NO_3^{-})H_2O$ and $(PRX^{+}Cl^{-})0.5H_2O$.

3.3. Thermal analysis

The thermal behavior of $(PRX^{+}NO_3^{-})H_2O$ was analyzed by DSC, TGA and HS microscopy. The DSC and TGA results are presented in Fig. 5. For comparative purposes, the DSC curve of $(PRX^{+}Cl^{-})0.5H_2O$ was also included in the plot. The DSC curve of PRX nitrate is characterized by an endothermic peak at 109.0 °C, attributed to the melting event. Also no dehydration event is observed for $(PRX^{+}NO_3^{-})H_2O$ until its melting, which can be seen as an advantage, since the stability of the drug is a basic requirement for their pharmaceutical development and manufacturability. The thermal decomposition appears in the DSC curve as an exothermic peak at ~169 °C and as expected, it is followed by an abrupt weight loss in the TGA curve. All thermal events assigned in the DSC curve were further confirmed by HS microscopy (Fig. 6). No habit or color change is observed for the nitrate salt between 25 and 80 °C. At 110 °C, the crystal starts to melt changing its morphology and above 112 °C, it has completely melting into a liquid droplet.

The melting temperature of PRX nitrate is about 24 °C less than the one found for $(PRX^{+}Cl^{-})0.5H_2O$ (Fig. 5). When compared with the $(PRX^{+}Cl^{-})H_2O$, in which the reported melting point is 117 °C [27–29], it shows a decrease of 15 °C. The melting point differences reinforces, among others supramolecular aspects, the differences in the nature of the CAHBs and consequently, in the lattice energy of these salts.

3.4. Solubility measurements

Equilibrium solubility is a thermodynamic parameter that shows the maximum amount of the solute dissolved in a given solvent at a specific temperature. From a pharmaceutical perspective, it constitutes an important parameter to the bioavailability of a drug. The water solubility of $(PRX^{+}Cl^{-})0.5H_2O$ and $(PRX^{+}NO_3^{-})H_2O$ was measured at 20 °C in deionized water. Despite our efforts, $(PRX^{+}Cl^{-})H_2O$ is a form difficult to obtain, and thus only the solubility of $(PRX^{+}Cl^{-})0.5H_2O$ hemihydrate, which is the formulation pharmaceutically approved, was determined. The solubility results for $(PRX^{+}NO_3^{-})H_2O$ and $(PRX^{+}Cl^{-})0.5H_2O$ are 4.01 mg mL^{-1} and 6.89 mg mL^{-1}, respectively, showing a decrease in the solubility of the nitrate salt in comparison with the chlorine one. In fact, the relative structural stability of these salts appears to be reflected in their solubility differences. Although the relationship between solubility and crystal structure is not so simple, it is well accepted that this process is associated with the ability of the salt to alter both the crystal lattice energy and the degree of solvation.

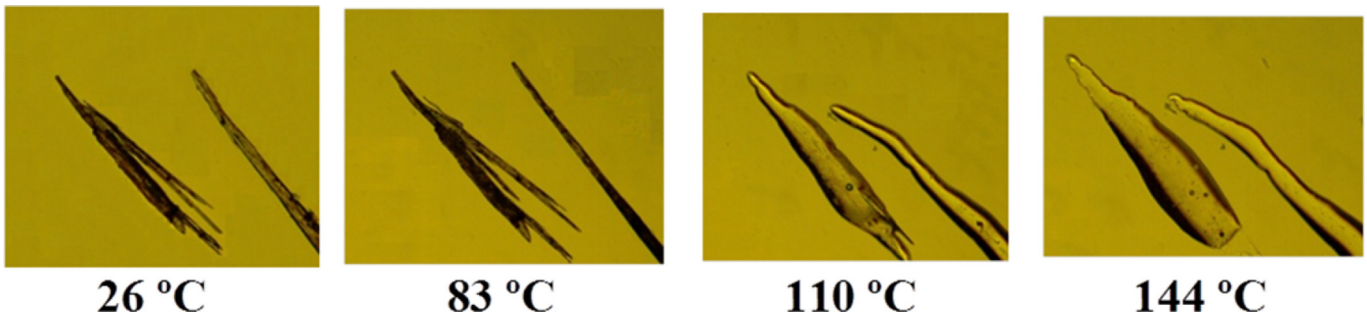

Fig. 6. Photomicrographs of the $(PRX^{+}NO_3^{-})H_2O$ under heat rate of 10 °C/min.

Following this assumption, since a larger molecular ion, like nitrate, is generally not as easy to solvate as a small one, it is plausible that $(PRX^{+}NO_3^{-})H_2O$ is less water soluble than $(PRX^{+}Cl^{-})0.5H_2O$.

4. Conclusions

In summary, the crystal structure of Paroxetine nitrate hydrate salt, $(PRX^{+}NO_3^{-})H_2O$, has been determined and its solid state characterization was performed using thermal analysis (DSC/TGA and HS Microscopy), FTIR spectroscopy and solubility measurements. Conformational similarity is observed between $(PRX^{+}NO_3^{-})H_2O$ and $(PRX^{+}Cl^{-})H_2O$ forms. The packing of PRX nitrate is essentially characterized by formation of ionic layers of PRX^{+} molecules connected to NO_3^{-} anions. In the crystal packing, these layers are intercalated by water channels. The presence of H_2O channels plays an important role in the supramolecular assembly of PRX^{+} NO_3^{-} ionic pairs, by reducing the electronic repulsion between the anions. The packing of $(PRX^{+}NO_3^{-})H_2O$ is also stabilized by C-H···O and C-H···π interactions. From a pharmaceutical perspective, this salt shows desirable properties for processing, storage and drug performance. There is no occurrence of any dehydration event and the structure is thermally stable between 25 and 100 °C. The present study shows that a better comprehension of the supramolecular features of PRX salts can be crucial for a successful development of a highly safe and efficient drug.

Acknowledgments

The authors would like to acknowledge Brazilian funding agencies FAPESP (P.S.C.-Jr. grant 12/05616-7), CAPES (C.C. M) and CNPq for financial support. Also, the authors would like to thanks Dr. Judith A. K. Howard Department of Chemistry, Durham University, UK for access to their X-ray facilities.

Appendix A. Supplementary data

Supplementary data related to this article can be found at http://dx.doi.org/10.1016/j.molstruc.2016.04.014.

References

[1] C. Hiemke, S. Härtter, Pharmacokinetics of selective serotonin reuptake inhibitors, Pharmacol. Ther. 85 (2000) 11–28.
[2] M. Bourin, P. Chue, Y. Guillon, Paroxetine: A Review, CNS Drug Rev. 7 (2001) 25–47.
[3] A.J. Goudie, W. Dubicki, M. Leathley, Paroxetine, a Selective 5-Hydroxytryptamine Uptake Inhibitor with Antidepressant Properties, Lacks Amphetamine-like Stimulus Properties in an Operant Drug Discrimination Bioassay in Rodents, J. Pharm. Pharmacol. 40 (1988) 192–196.
[4] M.B. Keller, Paroxetine Treatment of Major Depressive Disorder, 2003.
[5] M. Vaswani, F.K. Linda, S. Ramesh, Role of selective serotonin reuptake inhibitors in psychiatric disorders: a comprehensive review, Prog. Neuro Psychopharmacol. Biol. Psychiatry 27 (2003) 85–102.
[6] P. Blier, M. El Mansari, Serotonin and beyond: therapeutics for major depression, Philos. Trans. R. Soc. B Biol. Sci. 368 (2013).
[7] P.D. Bowen, Use of Selective Serotonin Reuptake Inhibitors in the Treatment of Depression in Older Adults: Identifying and Managing Potential Risk for Hyponatremia, Geriatr. Nurs. 30 (2009) 85–89.
[8] D.L. Prohotsky, F. Zhao, A survey of top 200 drugs—inconsistent practice of drug strength expression for drugs containing salt forms, J. Pharm. Sci. 101 (2012) 1–6.
[9] M.F. Pina, M. Zhao, J.F. Pinto, J.J. Sousa, C.S. Frampton, V. Diaz, O. Suleiman, L. Fábián, D.Q.M. Craig, An Investigation into the Dehydration Behavior of Paroxetine HCl Form I Using a Combination of Thermal and Diffraction Methods: The Identification and Characterization of a New Anhydrous Form, Cryst. Growth & Des. 14 (8) (2014) 3774–3782, http://dx.doi.org/10.1021/cg500150r.
[10] M. Yokota, Uekusa, Hidehiro, Ohashi, Yuji structure analyses of two crystal forms of paroxetine hydrochloride, Bull. Chem. Soc. Jpn. 72 (1999) 1731–1736.
[11] P.S. Carvalho, C.C. de Melo, A.P. Ayala, C.C.P. da Silva, J. Ellena, Reversible Solid-State Hydration/Dehydration of Paroxetine HBr Hemihydrate: Structural and Thermochemical Studies, Cryst. Growth & Des. 16 (2016) 1543–1549.
[12] S.M. Berge, L.D. Bighley, D.C. Monkhouse, Pharmaceutical salts, J. Pharm. Sci. 66 (1977) 1–19.
[13] D.P. Elder, R. Holm, H.L.d Diego, Use of pharmaceutical salts and cocrystals to address the issue of poor solubility, Int. J. Pharm. 453 (2013) 88–100.
[14] P.H. Stahl, C.G. Wermuth, I.U.o. Pure, A, Chemistry, Pharmaceutical Salts: Properties, Selection, and Use, Wiley, 2002.
[15] J. Wouters, L. Quere, D.E. Thurston, Pharmaceutical Salts and Co-crystals, Royal Society of Chemistry, 2011.
[16] Bruker, Saint, Bruker AXS Inc., Madison, Wisconsin, USA.
[17] Bruker, Sadabs, Bruker AXS Inc, Madison, Wisconsin, USA., 2001.
[18] O.V. Dolomanov, L.J. Bourhis, R.J. Gildea, J.A.K. Howard, H. Puschmann, OLEX2: a complete structure solution, refinement and analysis program, J. Appl. Crystallogr. 42 (2009) 339–341.
[19] G. Sheldrick, A short history of SHELX, Acta Crystallogr. Sect. A 64 (2008) 112–122.
[20] C.F. Macrae, P.R. Edgington, P. McCabe, E. Pidcock, G.P. Shields, R. Taylor, M. Towler, J. van de Streek, Mercury: visualization and analysis of crystal structures, J. Appl. Crystallogr. 39 (2006) 453–457.
[21] M. Harrass, C. Eirkson, C.M. Osbourne, P.G. Sayre, M. Zeeman, Water solubility, in: U.S.F.a.D. Administration (Ed.), Environmental Assessment Technical Assistance Handbook, 1987, pp. 1–11. Washington DC.
[22] J. Ibers, Paroxetine hydrochloride hemihydrate, Acta Crystallogr. Sect. C 55 (1999) 432–434.
[23] D. Cremer, J.A. Pople, General definition of ring puckering coordinates, J. Am. Chem. Soc. 97 (1975) 1354–1358.
[24] J.A.K. Howard, P. Pattison, O. Chetina, Private Communication to the Cambridge Crystallographic Data Centre, 2003.
[25] I.B. Cozar, L. Szabó, D. Mare, N. Leopold, L. David, V. Chiş, IR, Raman, SERS and DFT study of paroxetine, J. Mol. Struct. 993 (2011) 243–248.
[26] F.A. Miller, C.H. Wilkins, Infrared Spectra and Characteristic Frequencies of Inorganic Ions, Anal. Chem. 24 (1952) 1253–1294.
[27] M.F. Pina, J.F. Pinto, J.J. Sousa, L. Fábián, M. Zhao, D.Q.M. Craig, Identification and Characterization of Stoichiometric and Nonstoichiometric Hydrate Forms of Paroxetine HCl: Reversible Changes in Crystal Dimensions as a Function of Water Absorption, Mol. Pharm. 9 (2012) 3515–3525.
[28] G.V. Buxton, C.L. Greenstock, W.P. Helman, A.B. Ross, W. Tsang, Critical Review of rate constants for reactions of hydrated electronsChemical Kinetic Data Base for Combustion Chemistry. Part 3: Propane, J. Phys. Chem. Ref. Data 17 (1988), 513–513.
[29] N. Ward, V.W. Jacewicz, Paroxetine hydrochloride form A or C, Google Pat. (2000).